An *In-Vitro* Approach to Identifying Potential Drug Candidates to Prevent Acetaminophen Toxicity

A thesis submitted by

Vaughn Youngblood

in partial fulfillment of the requirements for the degree of

Master of Science

in

Pharmacology and Drug Development

Tufts University

May 2017

Adviser: David J. Greenblatt, MD

Abstract

Hepatic toxicity due to acetaminophen (APAP) is the leading cause of acute liver failure in the United States. Acetaminophen is largely metabolized by sulfotransferases and glucuronyl transferases. Once these enzymes are saturated, APAP is metabolized by CYP450 enzymes, particularly CYP2E1, into a hepatotoxic metabolite called N-acetyl-ρ-benzoquinone imine (NAPQI). Quantitatively measuring the accumulation of this toxic metabolite has been an elusive topic in previous literature. The analysis of the complex that NAPQI forms with hepatic glutathione (NAPQI-GSH) is the most reliable approach to quantitate metabolite formation. Using HPLC, incubations of increasing concentrations of APAP using human liver microsomes were performed in order to quantify toxic metabolite. To determine if the NADPH-regenerating system within the reaction was functioning as expected, incubations with midazolam, a benzodiazepine which undergoes CYP450 metabolism to hydroxylated metabolites, were performed

Concentrations of 2 µM, 5 µM, 20 µM, 50 µM, 200 µM, 500 µM, and 1mM APAP were used for incubations. Incubations consisted of NADPH-regenerating system including $NADP^+$, $MgCl_2$, sodium citrate, glucose-6-phosphate (G6P), and G6P dehydrogenase. Phosphate buffer and 1mM APAP (stock) were used as standards. Mobile phase consisted of 80% potassium phosphate (pH 2.2) and 20% methanol. A reverse-phase C18 column was used to analyze the products of the reactions (Waters Nova-Pak® C18 (4µm; 3.9x150mm)). UV absorbance was measured at 254nm. Midazolam incubations were analyzed using a Waters Nova-Pak® C18 (4µm; 3.9x150mm) HPLC column.

The NAPQI-GSH metabolite peak was not clearly defined with the specified method. HPLC analysis of APAP incubations yielded no significant metabolite peak formation. Further investigation using a similar HPLC method is needed.

Acknowledgements

Thank you to my parents, family, and friends who have been supporting me throughout my educational experience.

Table of Contents

List of Figures

List of Tables

List of Abbreviations

FDA – Food and Drug Administration

NSAIDs – Non-steroidal anti-inflammatory drugs

APAP – Acetaminophen

COX – Cyclooxygenase

NAPQI – N-acetyl-ρ-benzoquinone imine

HLM – Human liver microsomes

GSH - Glutathione

CYP450 – Cytochrome P450

DDC – Diethyldithiocarbamate

TNF-α – Tumor necrosis factor

IL-1β – Interleukin 1 beta

AST – Aspartate transaminase

ALT – Alanine aminotransferase

NF-κB – Nuclear factor kappa-light-chain-enhancer of activated B cells

An *In-Vitro* Approach to Identifying Potential Drug Candidates to Prevent Acetaminophen Toxicity

Chapter 1: Introduction

Acetaminophen (N-acetyl-*p*-aminophenol, APAP), also known by the brand name of Tylenol, is one of the most widely used antipyretic and analgesic over-the-counter medications (Ameer and Greenblatt, 1977). Compared to non-steroidal anti-inflammatory drugs (NSAID's) such as naproxen and ibuprofen, acetaminophen has a relatively low antipyretic effect. A common feature that both NSAIDs and other analgesic medications like acetaminophen share is the mechanism of pain relief. Both non-opioid analgesics inhibit COX enzymes that are involved in the regulation of pain and inflammation via the activation of pro-inflammatory cytokines called prostaglandins. These drugs particularly target COX-2, which are expressed mainly within inflamed tissues (Voloshyna et al., 2016). This specificity for COX-2 results in less gastric adverse effects as well. At therapeutic doses, APAP is often recommended as a first-line treatment for headaches, and the drug is safe and effective. However, upon overdose, severe liver damage can result that can be fatal (Hazai et al., 2002). Acetaminophen toxicity is the number one cause of acute liver failure in the US. The FDA advises not to take more than 4g of APAP per day. From 1990-1998, overdose of APAP was implicated in the cause of an estimated 56,000 emergency room visits, 26,000

hospitalizations, and 458 deaths (FDA: “Acetaminophen Overdose and Liver Injury”).

Once ingested, APAP is readily absorbed by the small intestine and metabolized in the liver. Due to this rapid absorption, APAP overdose is one of the most common causes of drug-induced hepatotoxicity in the US (Hazai et al., 2002) and leads to more calls to poison control centers in the US than any other pharmacologic substance (Lynch et al., 2007).

Phase of Toxicity	Clinical Presentation
Phase I: 0.5-24 hours after ingestion	Asympotmatic; nausea, vomiting
Phase II: 18-72 hours after ingestion	Upper right quadrant abdominal pain, nausea, vomiting, tachycardia, hypotension
Phase III: 72-96 hours after ingestion	Hepatic necrosis and dysfunction (jaundice, hepatic encephalopathy; continued nausea and vomiting

Figure 1.1: Clinical Presentations at Different Phases of APAP Toxicity

Source: Medscape (http://emedicine.medscape.com/article/820200-overview)

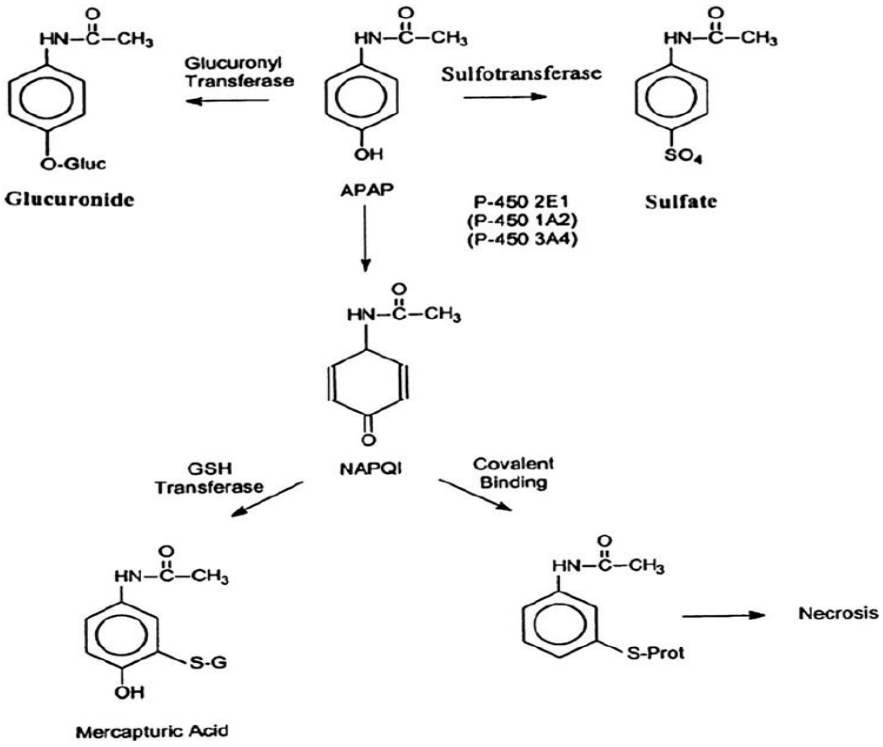

Figure 1.2: Metabolic pathway of APAP. Source: Larson et al., 2007

Drugs that undergo hepatic metabolism are acted upon by enzyme complexes, which can transform the drug to a more polar substance so that it can be excreted in the urine. These enzyme complexes are called cytochrome P450 (CYP450) enzymes. There are more than 50 different types of CYP enzymes which are expressed in various regions of the body besides the liver. However, only 6 of these types (CYP1A2, CYP2C9, CYP2C19, CYP2D6, CYP3A4, and CYP3A5) metabolize approximately 90% of drugs (Lynch et al., 2007). The metabolic transformation of APAP begins when the drug interacts with glucuronyl

transferase and sulfotransferase enzymes. Approximately 85-90% of a therapeutic dose of APAP undergoes sulfation and glucuronidation to form non-toxic, polar metabolites that are excreted in the urine. However, once these enzyme systems become saturated with APAP, the remaining amounts of the drug undergoes oxidation by hepatic cytochrome P-450 enzymes (mainly CYP2E1) to form a toxic, highly electrophilic intermediate, N-acetyl-*p*-benzoquinone imine (NAPQI) (Xie et al., 2016, Laine et al., 2009). At therapeutic doses of APAP, NAPQI is detoxified by forming a complex with glutathione (GSH), which is one of the principal antioxidants in the liver. With overdose of APAP, the available pool of glutathione is depleted, and the free NAPQI molecules can bind to hepatic proteins, causing oxidative stress and necrosis (Tan et al., 2008). Some individuals, such as liver disease patients and alcohol users, may be more susceptible to liver toxicity while taking acetaminophen (Wolf et al., 2007). In this case, toxicity can be reached in these individuals at lower doses than others (Lee, 2003). A reliable method of measuring NAPQI formation directly has not been developed, since NAPQI is very reactive. Thus, measuring the formation of NAPQI requires the quantification of the short-lived complex that NAPQI makes with GSH (NAPQI-GSH).

Toxic doses of APAP can also influence antioxidant activity in the liver. Oxidative stress can promote the activation of pro-inflammatory cytokines, such as TNF-α and IL-1β, which can further worsen APAP-induced hepatic injury. Upon metabolism of APAP into the NAPQI metabolite, there is an increase in circulating levels of both AST and ALT levels in the blood (El-Shafey et al., 2015).

Fortunately, there are treatments available that can decrease this inflammatory response and potentially prevent hepatic injury following toxic exposure to APAP. Currently, the first-line treatment for the reversal of hepatotoxicity caused by APAP is administration of oral or IV N-acetylcysteine. Acetylcysteine is a prodrug for L-cysteine, which is a precursor for the formation of GSH. Therefore, N-acetylcysteine administration has three main benefits: 1. Replenishes the available pool of GSH in the liver and prevents the expression of inflammatory cytokines such as NF-κB, 2. Blocks cyclooxygenase 2 (COX-2) signaling that would lead to the formation of inflammation-induced prostaglandins, and 3. Enhances conjugation and deactivation of NAPQI.

Recently, natural substances have been evaluated as an approach to modifying or preventing APAP toxicity. One of these is the flavonol compound, quercetin. Quercetin is commonly found in nature in sources such as apples, berries, and onions (Costa et al., 2016). This chemical acts as a scavenger of toxic free radicals and has potent anti-inflammatory actions. It has been suggested that quercetin can be co-administered with already-established anti-rheumatic drugs in the treatment of rheumatoid arthritis (Ji et al., 2013). An experimental in-vivo study showed that upon administration of quercetin after a single dose of APAP (3g/kg), mice showed significantly lower serum AST and ALT compared to mice given APAP alone (El-Shafey et al. 2015). Another in-vitro study showed that isoquercitrin, a derivative of quercetin, exhibited hepatoprotective and anti-inflammatory behavior when given prior to APAP administration (Xie et al., 2016).

This study also showed that when given alone, isoquercitrin inhibited CYP2E1 activity.

The objective of the current study is to investigate the role of CYP2E1 inhibition in the metabolism of APAP using human liver microsomes (HLM). At the same time, the mechanisms of action of several natural compounds including quercetin and green tea extract, which have similar antioxidant effects, will be investigated. To determine if there is a decrease in NAPQI formation upon APAP introduction, an inhibitor of CYP2E1 must be applied. Diethyl-dithiocarbamate (DDC) is the metabolite of the acetaldehyde dehydrogenase inhibitor, disulfiram. In addition to its role in the treatment of alcoholism, disulfiram and its metabolite are being suggested as an approach to treat hepatocellular carcinoma (HCC) (Goto et al., 2016, Wang et al., 2016). DDC inhibits NAPQI formation *in-vitro* more effectively than its parent drug (Goto et al. 2016).

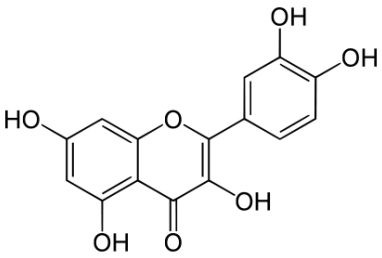

Quercetin

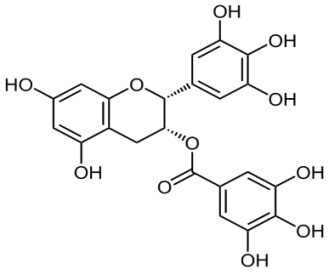

Green Tea Extract (epigallocatechin gallate)

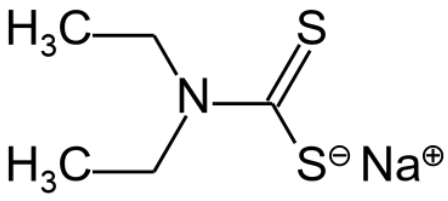

Sodium Diethyldithiocarbamate (DDC)

Chapter 2: Materials and Methods

2.1: Chemicals

Acetaminophen (APAP), glutathione (GSH), $NADP^+$, glucose-6 phosphate, glucose-6-phosphate dehydrogenase, sodium citrate, magnesium chloride, and DDC were all purchased from Sigma Aldrich. Potassium phosphate, methanol, and acetonitrile were purchased from Fisher Scientific. NAPQI was purchased from Cayman Chemical.

2.2: In-vitro metabolism of APAP

Varying concentrations of APAP (2, 5, 20, 50, 200, 500, and 1000uM) were placed in a vacuum centrifuge to yield a final incubation volume of 150µl. Cofactors used for energy production were $NADP^+$ (5mM), glucose-6-phosphate (3.3mM), glucose-6-phosphate dehydrogenase (5units/ml), sodium citrate (0.5mM), magnesium chloride (3.3mM), and glutathione (5mM) (**Table 1**). Human liver microsomes (HLM 866) (1mg/ml) were added with potassium phosphate buffer (50mM; pH 7.4) to yield a final reaction volume of 150µl.

Cofactor was incubated within a Blue M Magni Whirl constant temperature water bath set at 37°C for 5 minutes. After this, the cofactor was immediately placed in the vials containing dried APAP and placed in the 37°C water bath for 45 minutes. The reaction was stopped by the addition of 75ul of ice-cold acetonitrile and placed on ice for 2 minutes. Tubes were centrifuged for 10 minutes at 13,000rpm. Supernatant was withdrawn and analyzed by an Agilent 1200 HPLC instrument using a Nova-Pak® C18 (4um; 3.9x150mm) reverse phase column. Mobile phase,

which consisted of 80% potassium phosphate buffer (pH= 2.2) and 20% methanol, was delivered through the stationary phase under isocratic settings at a flow rate of 1ml/min, 254nm. The HPLC and column were washed with 100% methanol after each run sequence.

2.3: Cofactor Recipe

Reaction Volume (µL)	150			
N	5			
Ingredient	**Stock concentration**	**Desired final concentration**	**Volume per sample (µL)**	**Volume for batch (µL)**
NADP (make fresh) (mM)	10	0.5	7.5	37.5
MgCl2 (mM)	20	5	37.5	187.5
GSH (mM)	20	0	0	0
Na citrate (mM)	5	0.5	15	75
Glucose-6-phosphate (mM)	20	3.3	24.75	123.75
G6P-dehydrogenase (in units)	125	5	6	30
HLM (866) (µg/µL)	29.6	0.1	0.5	2.5
Phosphate buffer	50	n/a	58.7	293.7

Table 2.1: Listing of Cofactor Ingredients and Concentrations. $NADP^+$ stock is made fresh for each group of reactions.

The listed recipe is for a batch of six tubes, but the recipe changes accordingly with the number of tubes. NADP plays an important role in energy production through oxidation-reduction reactions. Another important molecule in this cofactor mix is glucose-6-phosphate dehydrogenase (G6PD). This enzyme is part of the pentose phosphate pathway, which is responsible for maintaining intracellular

levels of NADPH. Other components of the cofactor (sodium citrate, magnesium chloride ($MgCl_2$)) aid in maintaining pH balance and stability of the reaction.

For midazolam incubations, only 5mM $MgCl_2$ and 0.5mM $NADP^+$ are used. Glucose-6-phosphate and glucose-6-phosphate dehydrogenase are replaced by DL-isocitric acid and isocitric dehydrogenase respectively for midazolam incubations (von Moltke et al., 1996, von Moltke et al. 1996).

2.4: Midazolam Standards and Incubations

Midazolam (250µM; 150µl) was dried using a vacuum centrifuge. The cofactor ingredients used for these incubations were as follows: 0.05mM $NADP^+$, 3.75mM DL-isocitric acid, 1unit/ml isocitric dehydrogenase, 5mM Mg^{2+}, 0.5mg/ml HLM 866, and 50mM phosphate buffer (pH 7.7). The reactions were incubated for 5 minutes at 37°C. The reactions were passed through a Waters Nova-Pak® C18 (4µm; 3.9x150mm) reverse phase column and analyzed at a UV wavelength of 220nm.

2.5: HPLC conditions

HPLC analysis of standards and HLM incubations were conducted mainly under isocratic conditions. Gradient conditions were used only as described.

Chapter 3: Results

3.1: Controls

APAP and GSH reference standards were injected to establish their retention times **(Figure 3.1)** The GSH peak initially appeared at 3.4 minutes (A). However, after several weeks, the GSH peak had relocated to 2.1 minutes (B). The APAP peak relocated to 8.7 (C) minutes as compared to 4.2 minutes (D) initially. APAP and GSH reference standards were initially analyzed with a Waters µBondapak™ C18 (125A) reverse phase HPLC column (10µm; 3.9x300mm) column. Following the retention time shift, a Waters Nova-Pak® C18 (4µm; 3.9x150mm) column was used. This shift in retention time is expected when using a new column, especially one with a smaller diameter. This is also a factor when running samples over a period of time.

For analysis involving midazolam, the parent drug and its metabolites, 1-hydroxymidazolam and 4-hydroxymidazolam were processed as reference standards.

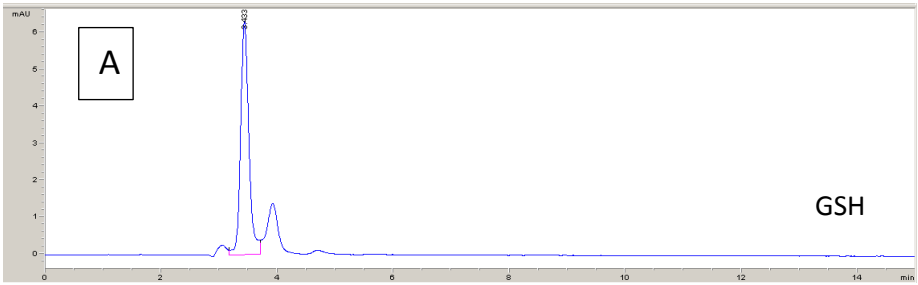

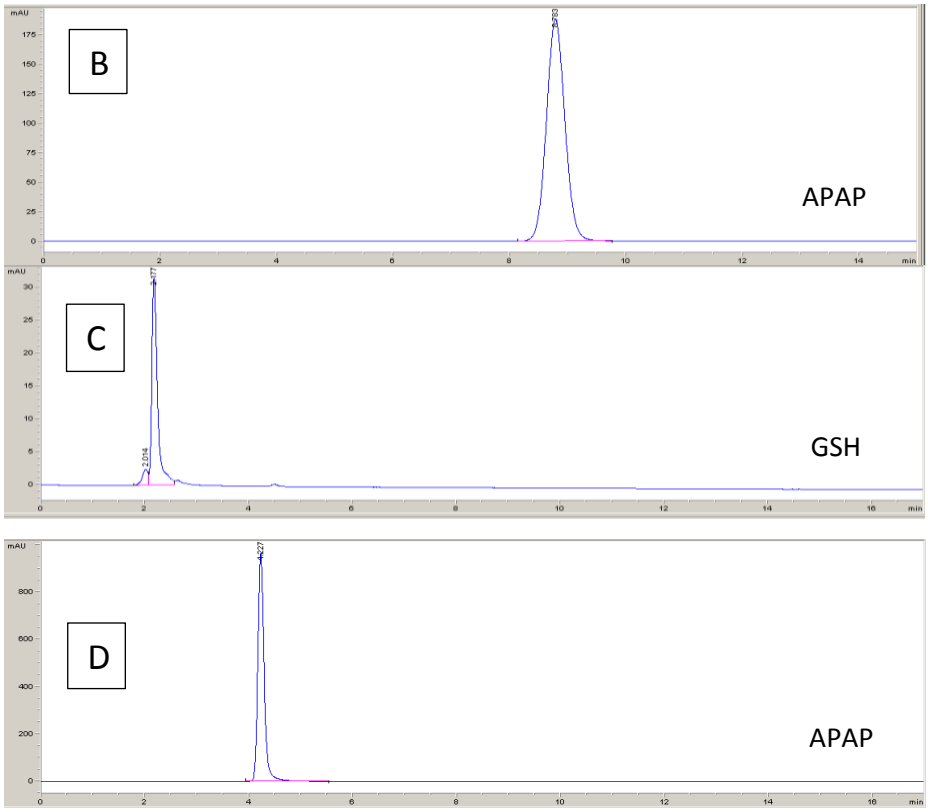

Figure 3.1: APAP and GSH reference standards. GSH (5mM) standards run a month apart. GSH and APAP controls (A, B) were analyzed using a Waters µBondapak™ C18 (125A) reverse phase HPLC column (10µm; 3.9x300mm). One month later, GSH and APAP controls (C, D) were analyzed using a Waters Nova-Pak® C18 (4µm; 3.9x150mm) reverse phase HPLC column.

NAPQI had more variation in both peak shape and retention time than other reference standards. In **Figure 3.2** below, you can see that when NAPQI is injected alone, the peak and retention time are both indistinct (**A**). Yet, one week later using the same column, the peak shape and retention time can be identified (**B**).

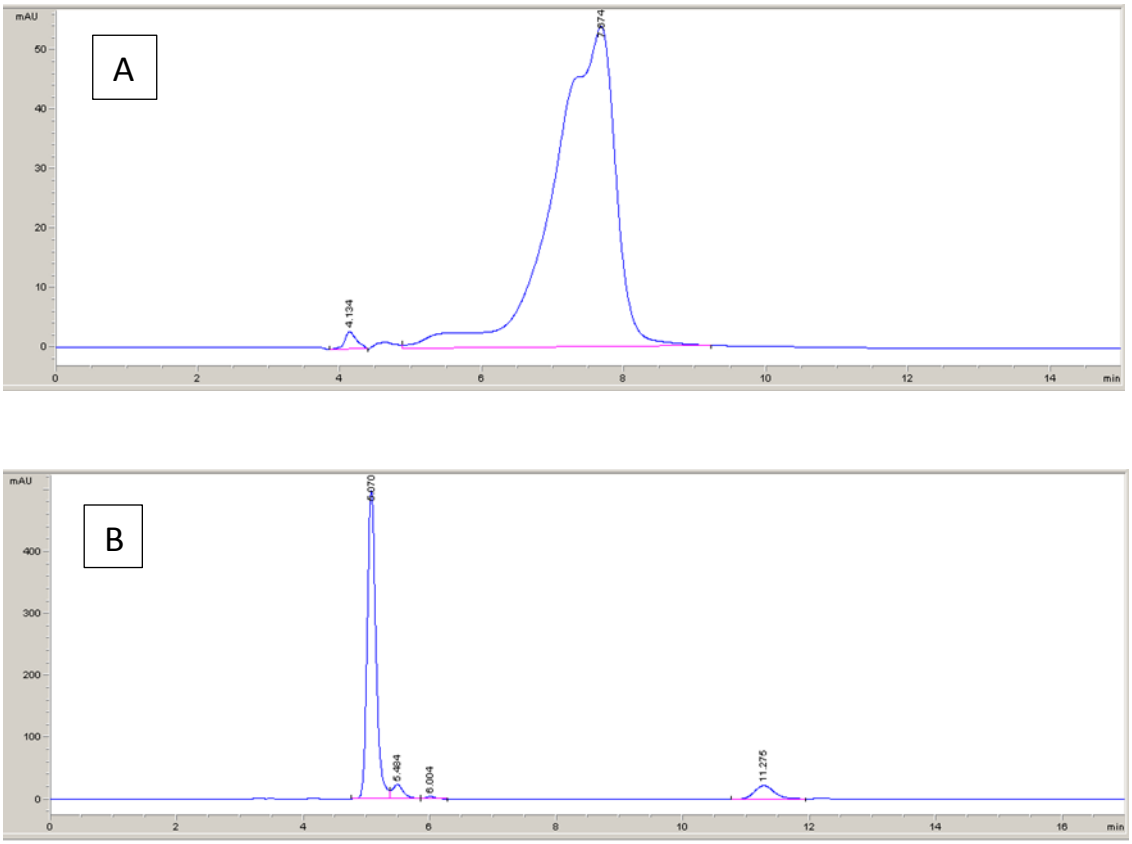

Figure 3.2: NAPQI controls using a Waters Nova-Pak® C18 (4µm; 3.9x150mm) reverse phase HPLC column. Top picture shows unclear results as to the retention time of the NAPQI peak (A), while the bottom picture shows a more distinct peak with several minor peaks (B). Both runs were performed one week apart while using the same column.

This leads to the next concept of identifying the NAPQI-GSH adduct. Unlike, the pure NAPQI control, this complex only forms during incubations with HLM and cofactors (Hazai et al., 2002). To evaluate this, incubations containing the same cofactor mixture and HLM as described before were performed. However, none of the peaks below (**Figure 3.3**) shows a clear indication of when this complex eluted, if at all.

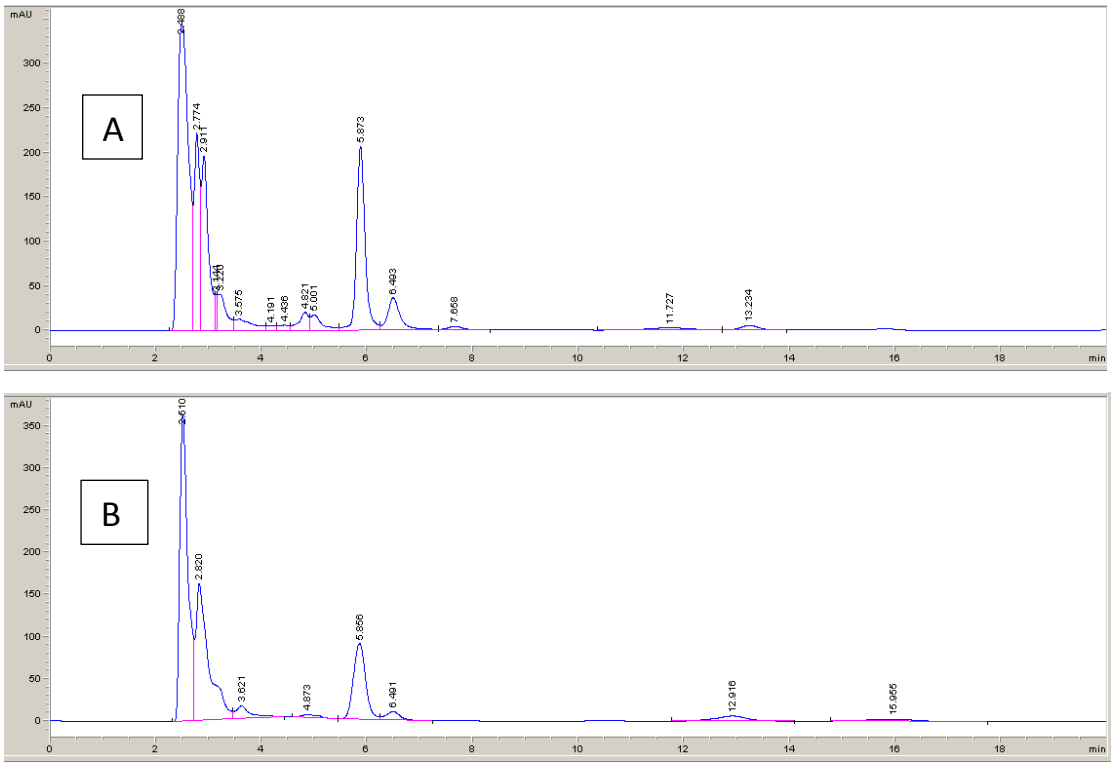

Figure 3.3: NAPQI-GSH formation. Reactions shown include HLM. Chromatograms showing no discernable difference in accuracy of isolating the NAPQI-GSH conjugate under incubation (A) and no incubation (B) conditions.

3.2: APAP Incubations with HLM

Using dried APAP and an incubation mixture designed to simulate hepatic metabolism *in-vivo*, reactions were performed to potentially identify the NAPQI-GSH complex. With increasing concentrations of APAP, it is expected that there would be increasing amounts of NAPQI (NAPQI-GSH) being formed from the reaction where it is present. As seen below (**Figure 3.4**), a peak formed at approximately 7.7 minutes which seemed to match the retention time for APAP that was mentioned in previous literature (Agarwal et al., 2011). As the concentration of APAP rose, the height of this peak rose as well.

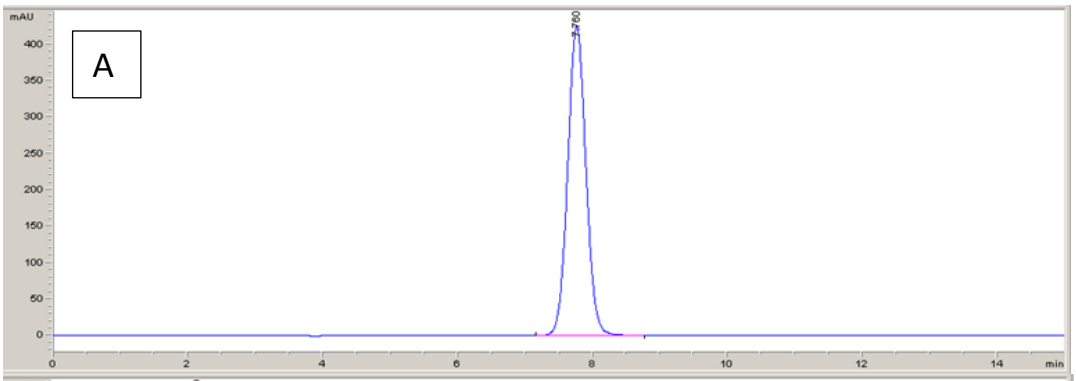
A
mAU
7.760
min

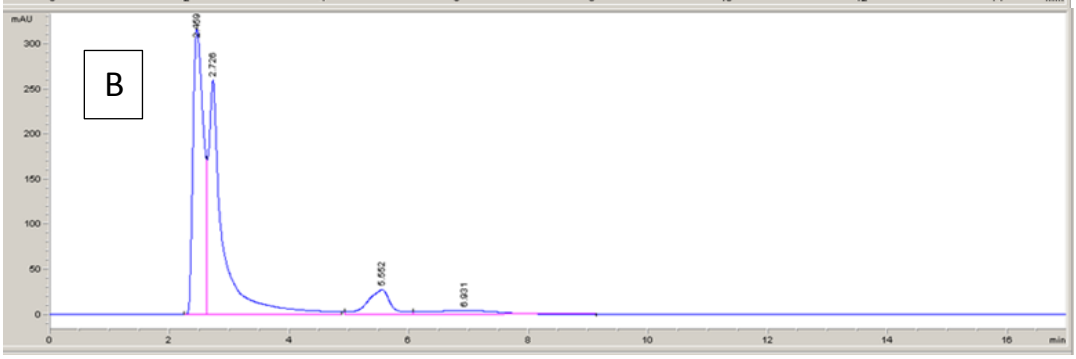
B
mAU
2.726
5.552
6.931
min

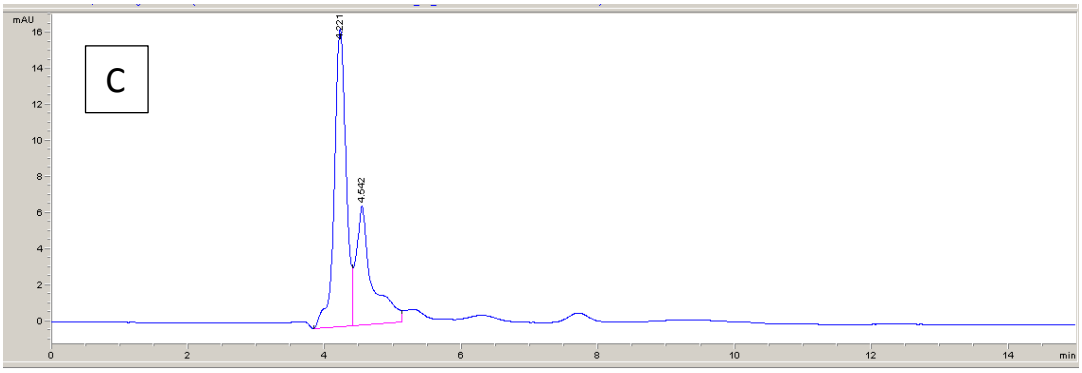
C
mAU
4.221
4.542
min

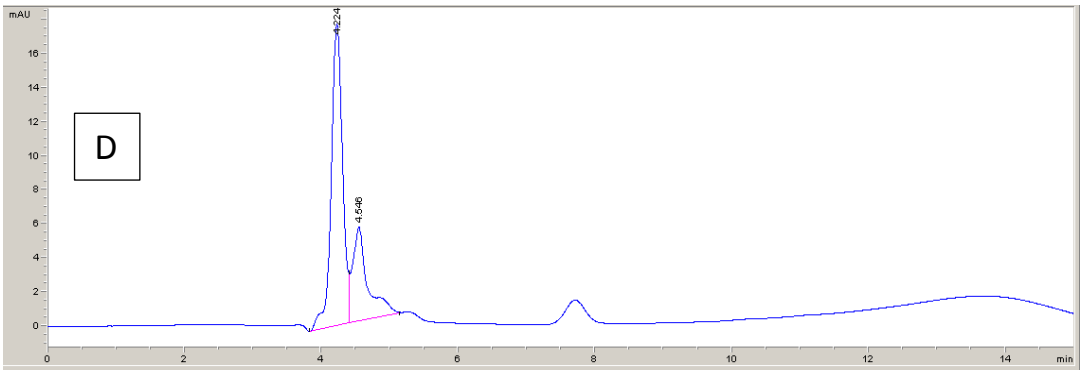
D
mAU
4.224
4.546
min

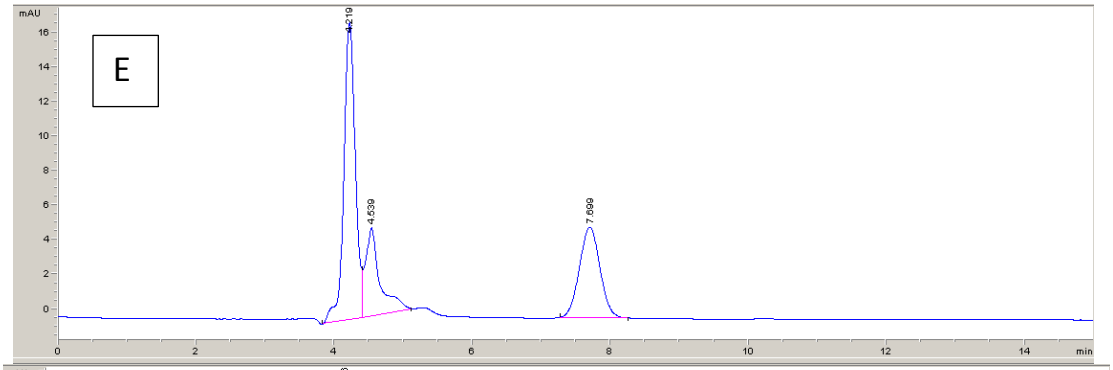
E
mAU
4.219
4.539
7.699
min

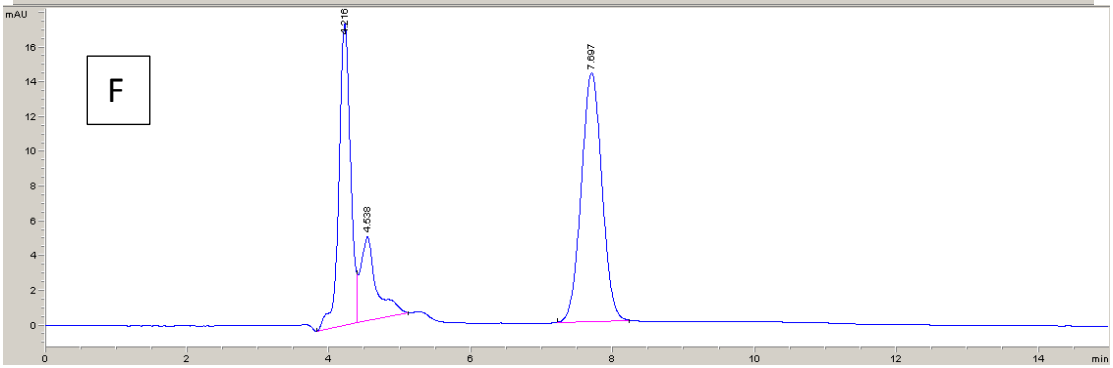
F
mAU
4.216
4.538
7.697
min

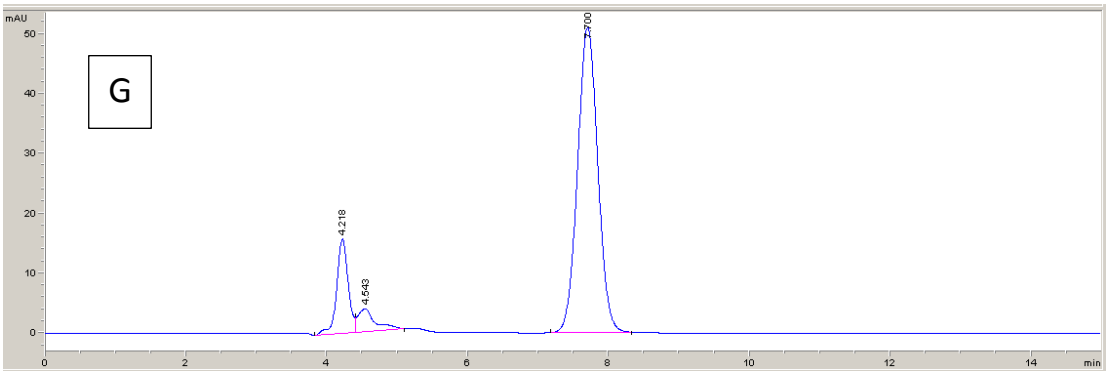
G
mAU
4.218
4.543
7.700
min

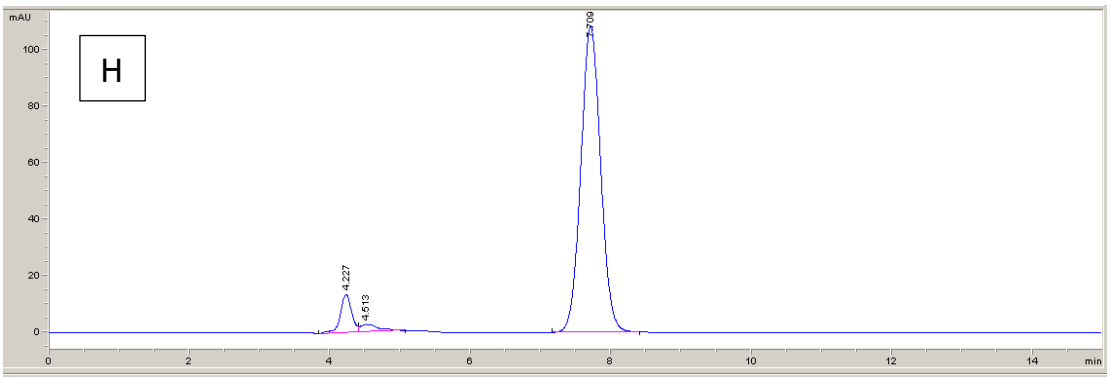
H
mAU
4.227
4.513
7.709
min

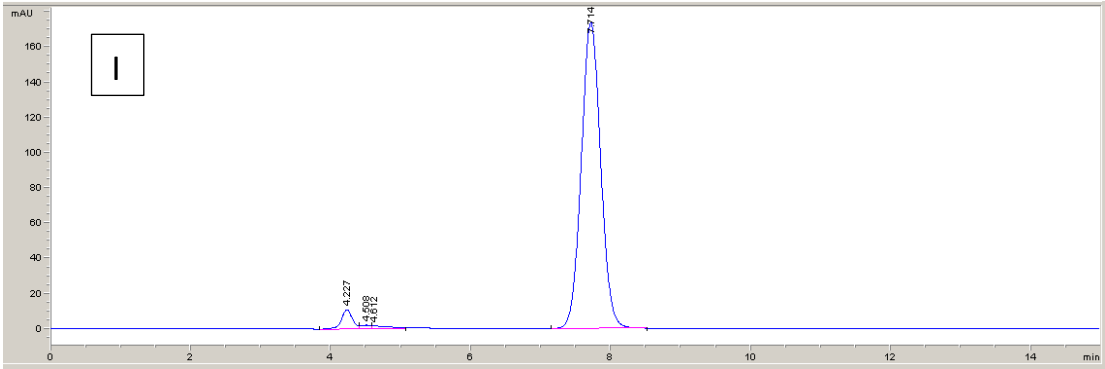

Figure 3.4: APAP incubations with HLM. APAP reference standard shown in A. APAP concentrations of 0µM (B), 2µM (C), 5µM (D), 20µM (E), 50µM (F), 200µM (G), 500µM (H), and 1mM (I) show an increasingly large peak on the chromatograph eluting at 7.7 minutes. The height of the peak which elutes at approximately 4 minutes does not change significantly. Y-axis is adjusted to fit peak height in each sample.

The elution time of the peak appearing at approximately 7.7 minutes overlaps with the elution time of the APAP standard which was injected on the same day. This would lead to the assumption that this peak corresponds to unreacted APAP. The elution time of this peak does not match the elution time of approximately 3.2 minutes that has been shown for NAPQI in previous literature (Florez-Perez, 2011).

3.3: Gradient versus Isocratic HPLC

The above APAP microsomal incubations were analyzed under isocratic HPLC conditions. Next, a gradient HPLC mobile phase was used to enhance clarity of metabolite peak formation.

Using 20mM potassium phosphate buffer and 100% methanol as the two separate mobile phases, the gradient for analysis is as follows: from 0-13 minutes, 3.5%

methanol; from 14-24 minutes, 17% methanol. Flow rate was 1ml/min and UV wavelength was 254nm. As shown in **Figure 3.5** below, the gradient method did not produce any additional benefit in identifying the NAPQI metabolite peak.

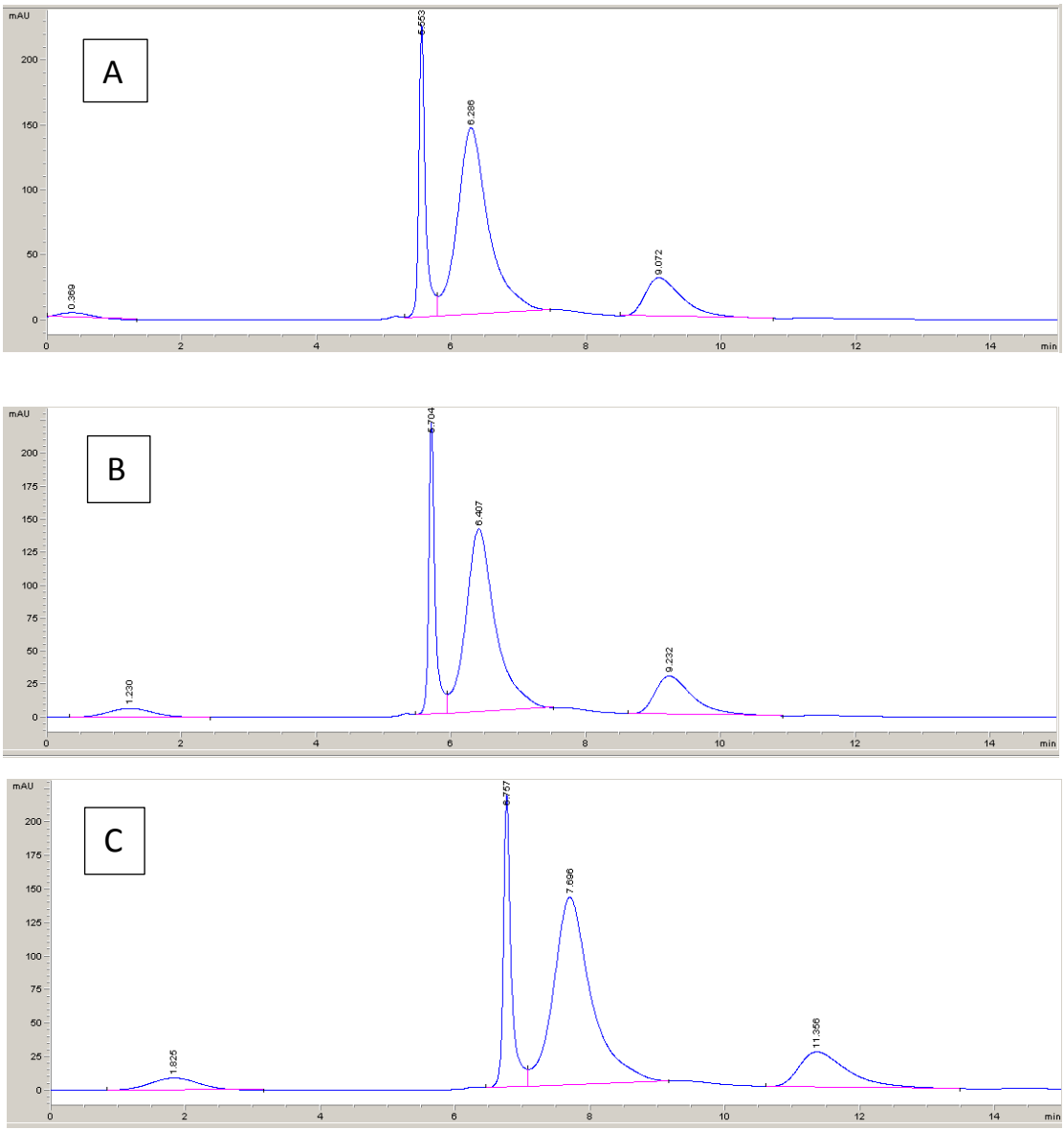

Figure 3.5: APAP incubations using gradient HPLC. APAP concentrations of 20µM (A), 50µM (B), and 200µM (C) are shown above. Samples were processed using a Waters Nova-Pak® C18 (4µm; 3.9x150mm) reverse-phase HPLC column.

3.4: Testing Column Efficiency

The results depicted in **Figure 3.2** illustrate the difference in results over time. Suspecting the possibility of degradation of the inner material within the column, and to eliminate the other possibility of peak shifting due to incorrect mixture of mobile phase, several repetitions of APAP and GSH injections were performed with a wash buffer (phosphate buffer (50mM)) separating them (**Figure 3.6**). Significant differences in peak retention time were noticed in between injections of the APAP and GSH reference standards.

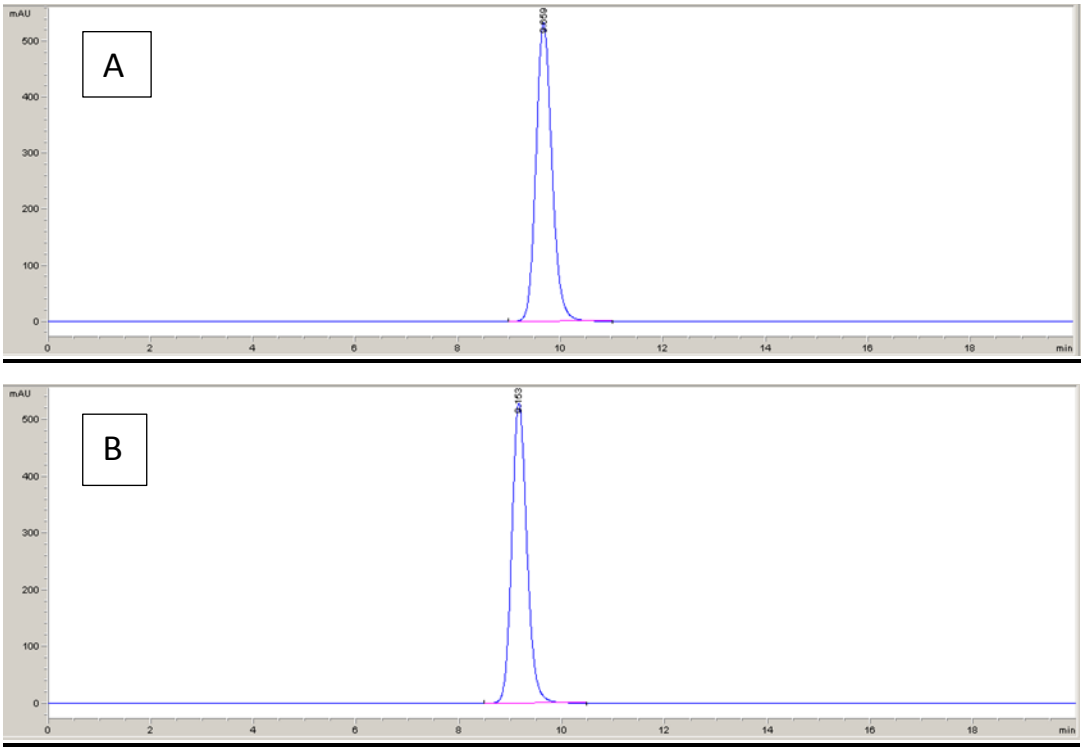

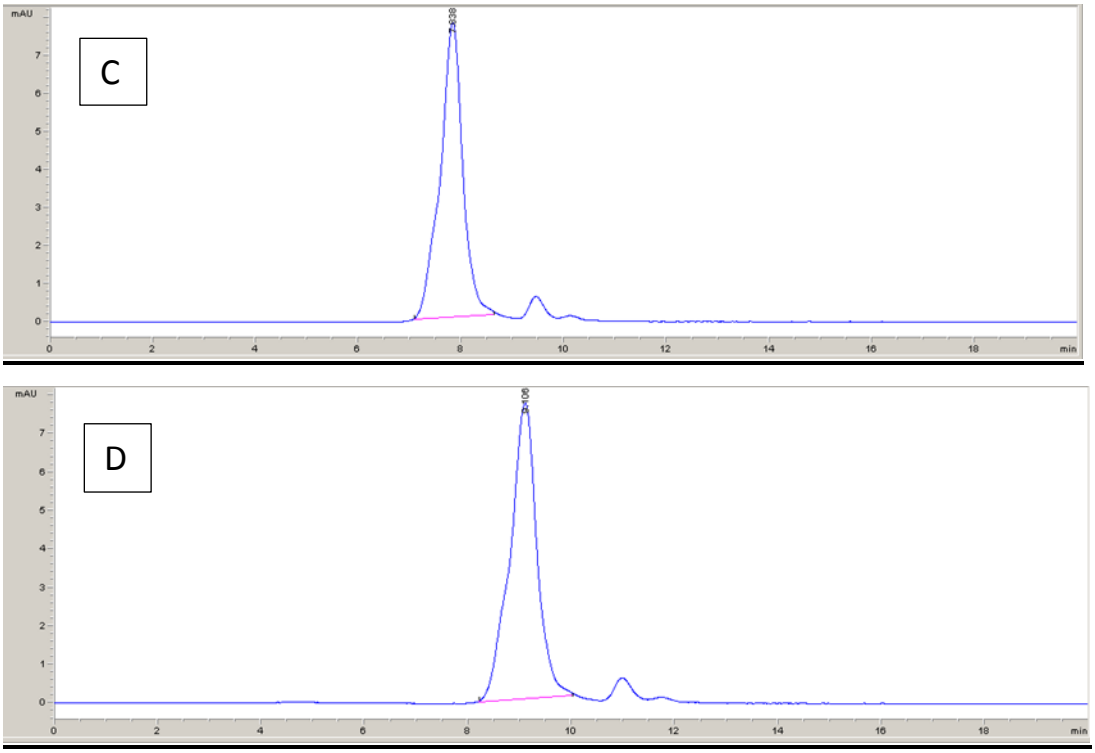

Figure 3.6: Testing HPLC Column Efficiency. APAP (A,B) and GSH (C,D) controls are shown. A sample of water was processed through the Waters Nova-Pak® C18 (4µm; 3.9x150mm) reverse-phase HPLC column after each consecutive control to evaluate elution efficiency.

3.5: HLM Incubations to Clarify Peak Representation

In an attempt to clearly identify the resultant peaks for each of the components involved in these incubations, HLMs were added in combination with these components. Up until this point, GSH has been included within the cofactor mixture and incubated with the other components. For this test, however, it was added separately to only the tubes which were designated to receive it. Looking at **Figure 3.7** below, no accurate peak representation can be made using the current method.

Sample	Contents of Sample
A	HLM+Phosphate Buffer
B	HLM+Cofactor
C	HLM+Cofactor+APAP
D	HLM+APAP
E	HLM+GSH
F	HLM+GSH+Cofactor
G	HLM+GSH+APAP
H	HLM+GSH+APAP+Cofactor

Table 3.1: Sample layout for HLM test incubations

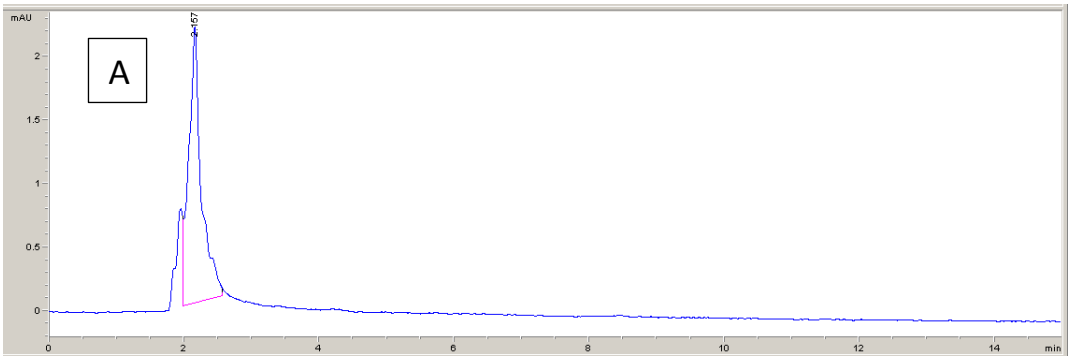

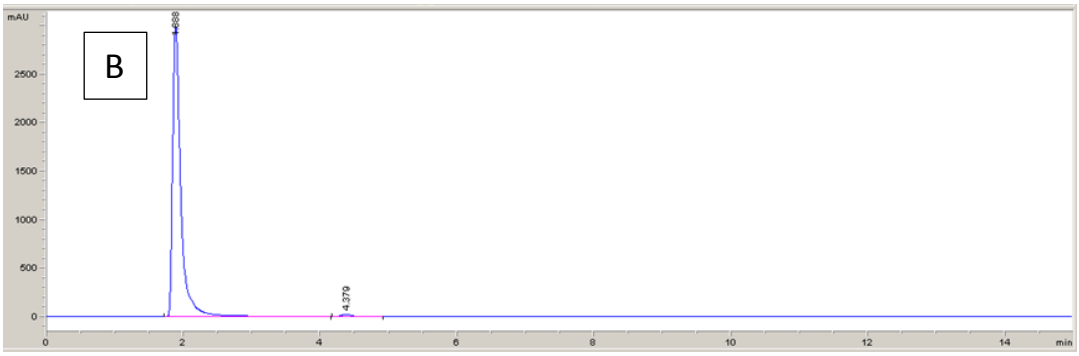

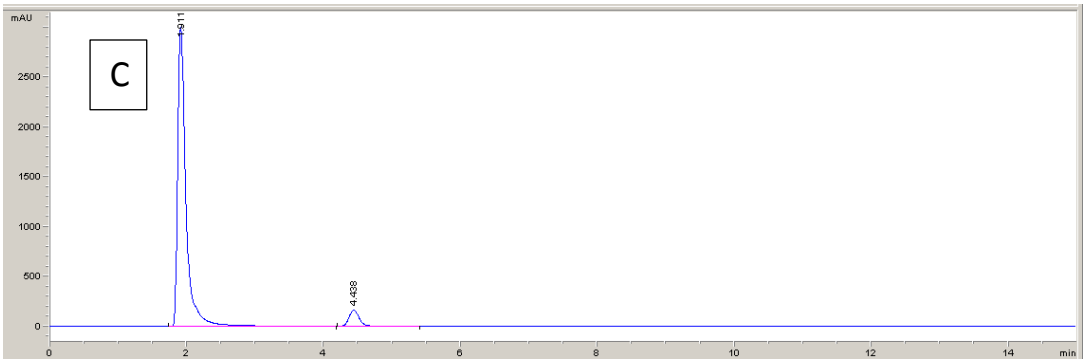

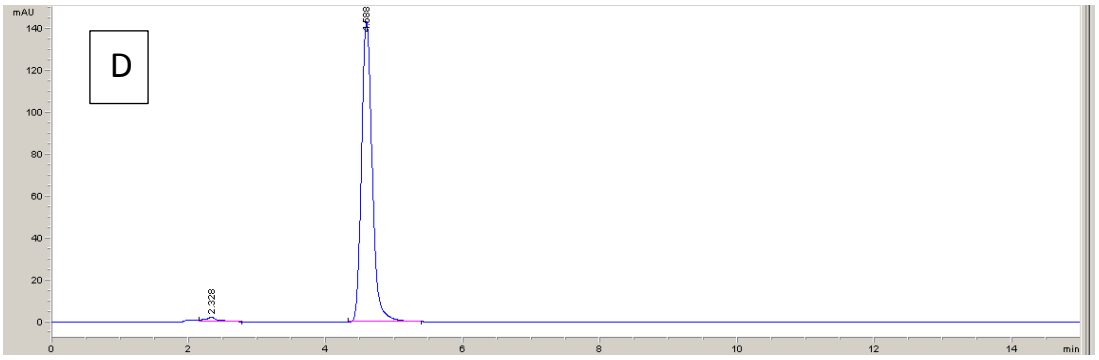
D
mAU
140
120
100
80
60
40
20
0
2.328
4.688
0
2
4
6
8
10
12
14
min

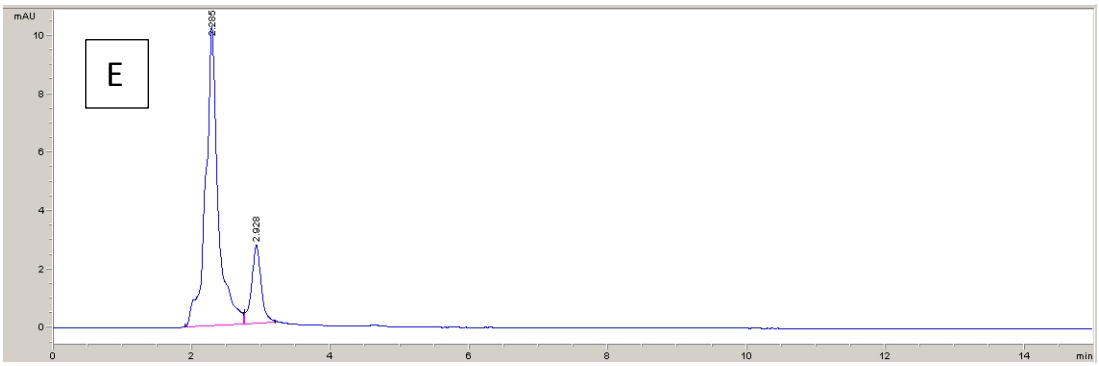
E
mAU
10
8
6
4
2
0
2.285
2.928
0
2
4
6
8
10
12
14
min

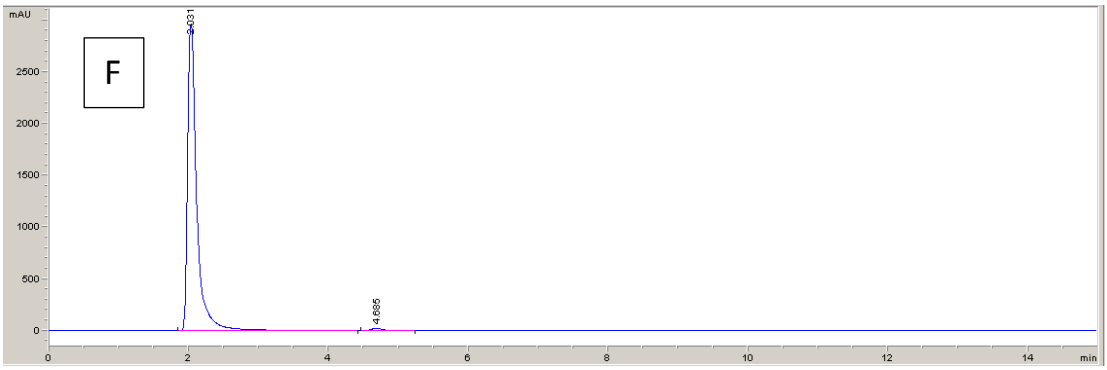
F
mAU
2500
2000
1500
1000
500
0
2.031
4.685
0
2
4
6
8
10
12
14
min

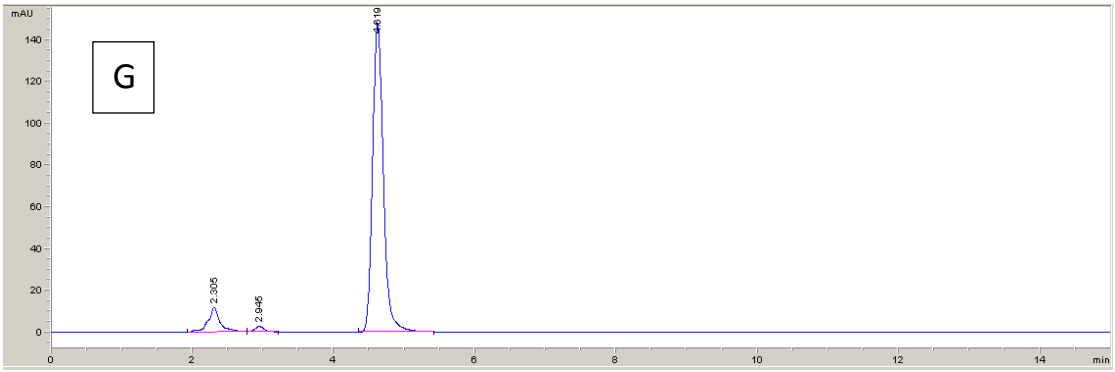
G
mAU
140
120
100
80
60
40
20
0
2.305
2.945
4.619
0
2
4
6
8
10
12
14
min

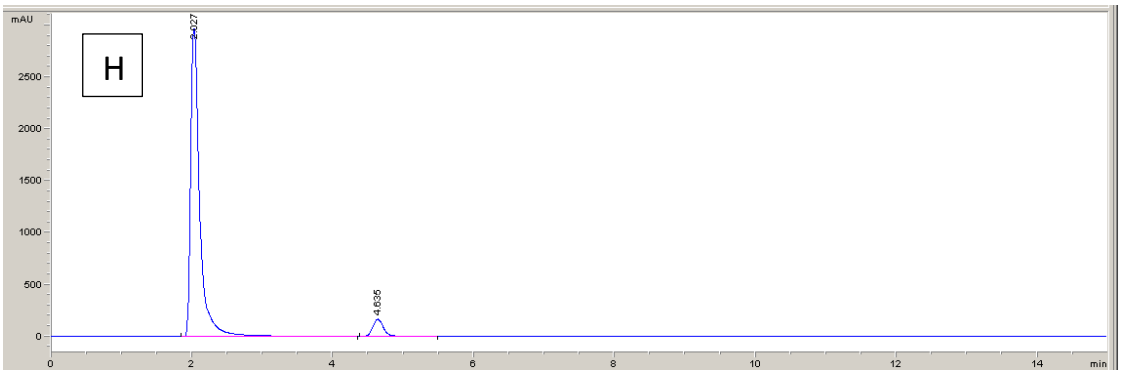

Figure 3.7: HLM Testing. Incubations of HLM with other components of APAP reaction.The incubations were as follows: HLM + phosphate buffer only (A), HLM + cofactor (B), HLM + cofactor + APAP (C), HLM + APAP (D), HLM + GSH (E), HLM + GSH + cofactor (F), HLM + GSH + APAP (no cofactor) (G), and HLM + GSH + APAP + cofactor (H). The scale of the Y-axis is adjusted according to peak height for each sample

3.6: Midazolam Reference Standards and Incubations

In order to verify the metabolic activity of the HLM (in that, CYP2E1), reference standards and incubations using midazolam, a benzodiazepine mostly metabolized by CYP3A4, were evaluated (**Figure 3.8**). Midazolam theoretically is metabolized and converted into its metabolites 1-hydroxymidazolam and 4-hydroxymidazolam. However, looking at the resulting chromatograms, no metabolite peaks are visible. The retention time of the reference peak for midazolam (250µM) is different from the retention time of midazolam for the incubation samples.

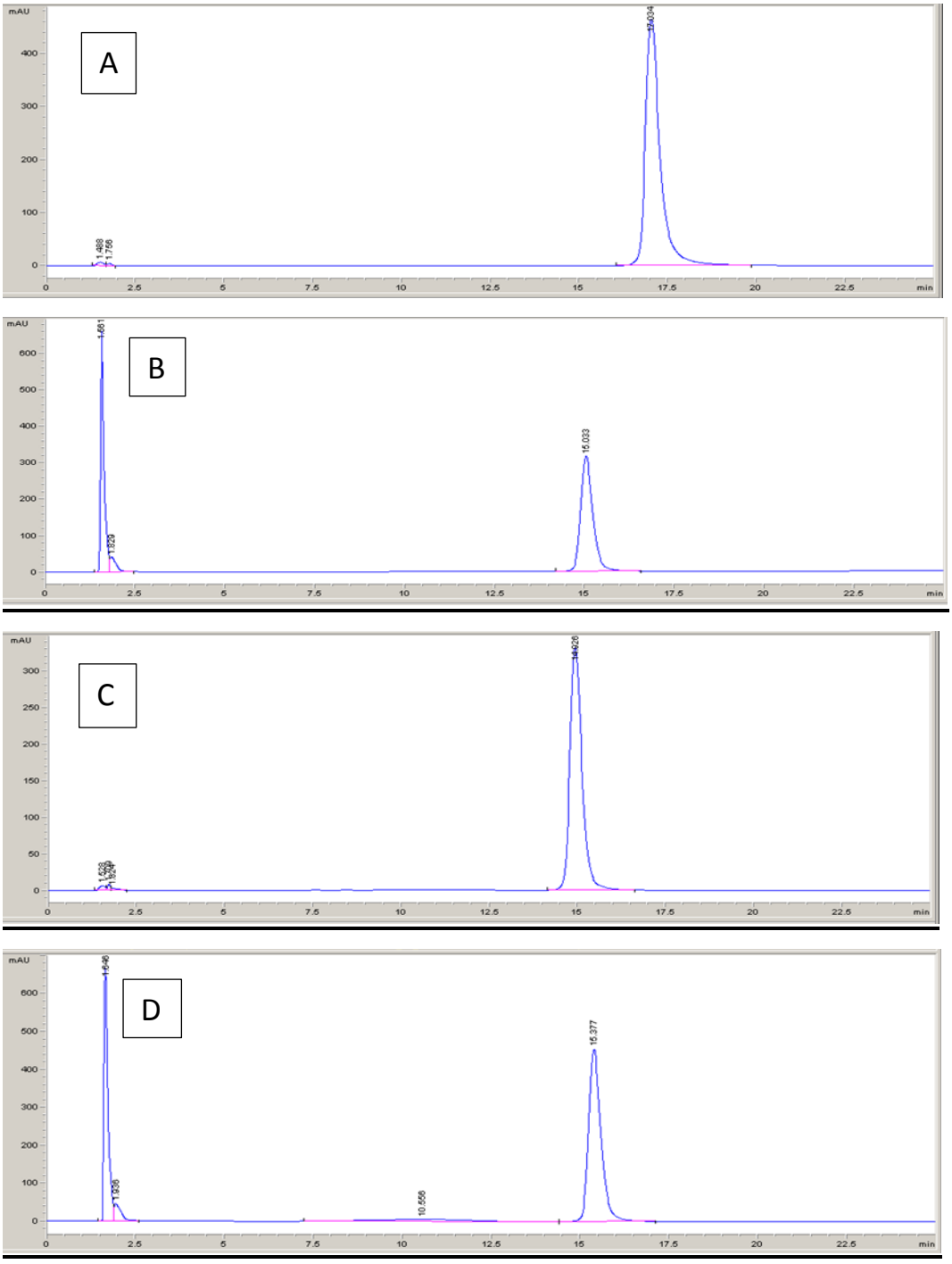

Figure 3.8: Midazolam Standards and Incubations. (A) Midazolam reference standard (250µM); (B) Incubation of cofactor mix and midazolam; (C) Incubation of HLM (in 50mM phosphate buffer) with midazolam; (D) Incubation containing HLM, cofactor mix, and midazolam.

Chapter 4: Discussion

High pressure liquid chromatography (HPLC) uses high pressure to deliver a sample mixture through a separation column. As solvent is passed through a column, compounds within the sample move at different rates due to their differential affinities (polar versus nonpolar interactions) for the stationary phase. Typically, either silica or carbon beads are packed into the column. The solvent containing the compound of interest is termed the mobile phase. Typically, mobile phase can include a combination of organic (acetonitrile, methanol) and aqueous (KH_2PO_4) liquids. The mobile phase components can be adjusted depending on the polarity of the desired compound to be measured. To elute a polar compound within the mobile phase, the column should contain nonpolar material (carbon). To elute a nonpolar component, the column should be packed with polar material (silica beads). Once a compound is eluted from the column, it passes through a UV detector which absorbs a signal proportional to the amount of analyte in the mobile phase. The instrument processes this signal in the form of peaks that appear at constant retention times (the duration of time taken to pass through the HPLC column). The height or area of these peaks is proportional to the quantity of the compound in the eluent (Source: Waters®)

Hepatic cytochrome P450 enzymes are responsible for the metabolism and transformation of many different compounds, some of which can be more reactive and harmful in their transformed state as compared to their original state. These enzymes are membrane-bound to the cell (cyto-) and they contain a heme pigment (chrome and P), which absorbs light at a wavelength of 450nm in the presence of

carbon monoxide (CO) (Lynch et al., 2007). Investigators have used human liver microsomes for the analysis of NAPQI-GSH formation previously (Chen et al., 1998). Other studies have used mouse liver microsomes to identify the formation of the NAPQI-GSH conjugate (Tan et al., 2008).

Gradient HPLC is useful when the components of the elution mixture vary in terms of polarity. Unlike with isocratic HPLC, gradient HPLC involves more than one mobile phase; organic and aqueous components are mixed prior to passage through the reverse-phase column. The mixture of mobile phases is customized to achieve an increase in organic solvent concentration over the course of analysis.

The indistinct NAPQI peak in **Figure 3.2** was thought to be due to column degradation since both samples were analyzed with the same column one week apart. However, upon re-evaluation with a new column, the peak formation became more distinct yet did not provide a replicable retention time for pure NAPQI (**B**). At this point, the flow rate was changed from 1.0ml/min to 1.3ml/min to determine if the faster flow rate would help elution of metabolite. This did not change the clarity of the NAPQI peak.

The APAP-GSH incubations with HLM yield two noticeable peaks with retention times of approximately 4 and 7.5 minutes. The peak at 4 minutes likely corresponds to most (or all) of the compounds within the incubation cofactor. The peak at 7.5 minutes likely corresponds to APAP, since the APAP reference standard eluted at approximately that time and the height of this peak rises with increasing concentrations of APAP.

As mentioned before, once the NAPQI metabolite is formed, it can either bind to the inner lining of the liver or form a complex with GSH which can be easily excreted in the urine. Quantifying NAPQI metabolite formation involves measuring the NAPQI-GSH conjugate. A distinctive peak for NAPQI-GSH was not obtained using either isocratic or gradient HPLC techniques. Altering the concentration of the energy-producing component of the cofactor ($NADP^+$) did not have an effect on the product yield.

The batch of incubations in Figure 3.4 were conducted on the same day and analyzed using the same HPLC conditions as mentioned earlier. The peak at a retention time of 7.7 minutes which gradually increases in height is assumed to be the APAP reference standard peak. Given the inaccurate results of the pure NAPQI standard, it is difficult to make any conclusions as to the formation of the NAPQI metabolite or if it forms at all. This can be a subject of further investigation.

One part of this protocol that needs more attention is the energy-producing system that drives the reaction. It seems that the only discernable result that has potential to be investigated further is in **Figure 3.4** showing a peak whose height is increasing with increasing APAP concentrations. The fact that the NAPQI metabolite formation *in-vivo* is relatively low compared to other, less harmful metabolites must be taken into account. In conclusion, looking at the chromatograms from incubations with HLM, APAP, and midazolam, the resultant peaks are indistinct and do not yield definite production of the NAPQI metabolite.

Acetaminophen is widely used for its analgesic properties, so eliminating any risks associated with its use would be highly beneficial. Quercetin and green

tea extract have antioxidant properties and serve to protect the body from stress and organ damage.

Due to time constraints, analysis of the effect of DDC and green tea extract on the metabolic activity of CYP2E1 enzymes using HPLC was not established. These experiments, however, lay the foundation for further investigation into the quantification of the NAPQI metabolite. Given how commonly acetaminophen is used, new information in regards to what can prevent hepatic toxicity upon repeated acetaminophen doses is important and can have a significant health impact.

Chapter 5: Bibliography

1-23

1. Agarwal R, MacMillan-Crow LA, Rafferty TM, et al. Acetaminophen-Induced Hepatotoxicity in Mice Occurs with Inhibition of Activity and Nitration of Mitochondrial Manganese Superoxide Dismutase. *The Journal of Pharmacology and Experimental Therapeutics*. 2011;337(1):110-118.

2. Ameer B, Greenblatt DJ. Acetaminophen. Annals of internal medicine 1977; 87: 202-09

3. Chen C, Krausz KW, Idle JR, Gonzalez FJ. Identification of novel toxicity-associated metabolites by metabolomics and mass isotopomer analysis of acetaminophen metabolism in wild-type and Cyp2e1-null mice. The Journal of biological chemistry 2008;283:4543-59.

4. Chen W, Koenigs LL, Thompson SJ, et al. Oxidation of acetaminophen to its toxic quinone imine and nontoxic catechol metabolites by baculovirus-expressed and purified human cytochromes P450 2E1 and 2A6. Chemical research in toxicology 1998;11:295-301.

5. Costa LG, Garrick JM, Roque PJ, Pellacani C. Mechanisms of Neuroprotection by Quercetin: Counteracting Oxidative Stress and More. Oxidative medicine and cellular longevity 2016;2016:2986796.

6. El-Shafey MM, Abd-Allah GM, Mohamadin AM, Harisa GI, Mariee AD. Quercetin protects against acetaminophen-induced hepatorenal toxicity by reducing reactive oxygen and nitrogen species. Pathophysiology : the official journal of the International Society for Pathophysiology 2015;22:49-55.

7. Flores-Perez C, Chavez-Pacheco JL, Ramirez-Mendiola B, et al. A reliable method of liquid chromatography for the quantification of acetaminophen and identification of its toxic metabolite N-acetyl-p-benzoquinoneimine for application in pediatric studies. Biomedical chromatography : BMC 2011;25:760-6.

8. Forrest JA, Clements JA, Prescott LF. Clinical pharmacokinetics of paracetamol. Clinical Pharmacokinetics 1982;7:93-107.

9. Goto K, Kato N, Chung RT. Anti-hepatocellular carcinoma properties of the anti-alcoholism drug disulfiram discovered to enzymatically inhibit the AMPK-related kinase SNARK in vitro. Oncotarget 2016;7:74987-99.

10. Hazai E, Vereczkey L, Monostory K. Reduction of toxic metabolite formation of acetaminophen. Biochemical and biophysical research communications 2002;291:1089-94.

11. James LP, Mayeux PR, Hinson JA. Acetaminophen-induced hepatotoxicity. Drug metabolism and disposition: the biological fate of chemicals 2003;31:1499-506.

12. Ji JJ, Lin Y, Huang SS, Zhang HL, Diao YP, Li K. Quercetin: a potential natural drug for adjuvant treatment of rheumatoid arthritis. African journal of traditional, complementary, and alternative medicines : AJTCAM 2013;10:418-21.
13. Laine JE, Auriola S, Pasanen M, Juvonen RO. Acetaminophen bioactivation by human cytochrome P450 enzymes and animal microsomes. Xenobiotica 2009;39(1): 11-21.
14. Larson AM. Acetaminophen hepatotoxicity. Clinics in liver disease 2007;11:525-48, vi.
15. Larson AM, Polson J, Fontana RJ, et al. Acetaminophen-induced acute liver failure: results of a United States multicenter, prospective study. Hepatology (Baltimore, Md) 2005;42:1364-72.
16. Lee W. Drug-induced hepatotoxicity, New England Journal of Medicine, July 31, 2003; 349:474-485
17. Lynch T, Price A. The effect of cytochrome P450 metabolism on drug response, interactions, and adverse effects. American family physician 2007;76:391-6.
18. Manyike PT, Kharasch ED, Kalhorn TF, Slattery JT. Contribution of CYP2E1 and CYP3A to acetaminophen reactive metabolite formation. Clinical pharmacology and therapeutics 2000;67:275-82.
19. Nourjah P, Ahmad SR, Karwoski C, Willy M. Estimates of acetaminophen (Paracetamol)-associated overdoses in the United States. Pharmacoepidemiology and drug safety 2006;15:398-405.
20. Reilly TP, Brady JN, Marchick MR, et al. A protective role for cyclooxygenase-2 in drug-induced liver injury in mice. Chemical research in toxicology 2001;14:1620-8.
21. Rowden AK, Norvell J, Eldridge DL, Kirk MA. Updates on acetaminophen toxicity. The Medical clinics of North America 2005;89:1145-59.
22. Tan SC, New LS, Chan EC. Prevention of acetaminophen (APAP)-induced hepatotoxicity by leflunomide via inhibition of APAP biotransformation to N-acetyl-p-benzoquinone imine. Toxicology letters 2008;180:174-81.
23. Voloshyna I, Kasselman LJ, Carsons SE, et al. COX-2-dependent and independent effects of COX-2 inhibitors and NSAIDs on proatherogenic changes in human monocytes/macrophages. Journal of investigative medicine 2017; 65(3); 694-704.
24. von Moltke LL, Greenblatt DJ, Harmatz JS, et al. Triazolam biotransformation by human liver microsomes in vitro: effects of metabolic inhibitors and clinical confirmation of a predicted interaction with ketoconazole. The Journal of pharmacology and experimental therapeutics 1996;276:370-9.
25. von Moltke LL, Greenblatt DJ, Schmider J, et al. Midazolam hydroxylation by human liver microsomes in vitro: inhibition by fluoxetine, norfluoxetine, and by azole antifungal agents. Journal of clinical pharmacology 1996;36:783-91.
26. Wang Z, Tan J, McConville C, et al. Poly lactic-co-glycolic acid controlled delivery of disulfiram to target liver cancer stem-like cells. Nanomedicine : nanotechnology, biology, and medicine 2016; 13; 641-657.
27. Wolf KK, Wood SG, Allard JL, Hunt JA, Gorman N, Walton-Strong BW, Szakacs JG, Duan SX, Court MH, von Moltke LL, Greenblatt DJ, Kostrubsky V, Jeffery EH, Wrighton SA, Gonzalez FJ, SInclair PR, Sinclair JF. Role of CYP3A and CYP2E1 in alcohol-mediated increases in acetaminophen hepatotoxicity: comparison of wild-type and CYP2e1(-/-) mice. Drug Metabolism and Disposition 2007; 35: 1223-1231.
28. Xie W, Wang M, Chen C, Zhang X, Melzig MF. Hepatoprotective effect of isoquercitrin against acetaminophen-induced liver injury. Life sciences 2016;152:180-9.